Biochimica et Biophysica Acta, 777 (1984) 297–305
Elsevier

BBA 72342

SLOW-MOTION ESR OF CHOLESTANE SPIN LABELS IN PLANAR MULTIBILAYERS OF DIACYLDIGALACTOSYLDIGLYCERIDES

PAUL KOOLE, A.J. DAMMERS, GIJS VAN GINKEL and YEHUDI K. LEVINE *

Department of Biophysics, Physics Laboratory, University of Utrecht, Princetonplein 5, 3584 CC Utrecht (The Netherlands)

(Received May 7th, 1984)

Key words: Cholestane spin label; Planar multibilayer; Diacyldigalactosyldiglyceride; ESR; (Chloroplast membrane)

The orientation and restricted motion of the cholestane spin label (3-spiro-doxyl-5α-cholestane) incorporated into planar multibilayers of diacyldigalactosyldiglycerides extracted from the thylakoid membranes of chloroplasts from different plant leaves has been studied. The experimental ESR spectra were simulated in terms of the slow-tumbling ESR formalism of Freed and co-workers (Polnaszek, C.F., Bruno, G.V. and Freed, J.H. (1973) J. Chem. Phys. 58, 3185–3199). The analysis shows that the degree of orientational order is low. The spin label molecules undergo a faster reorientational motion about their long molecular axes than perpendicular to them. At room temperature the reorientational rate around the long molecular axis falls within the fast-motional limit, while the reorientation rate of the long axis itself corresponds to the slow-tumbling regime. The results indicate that the motion of the labels in bilayers of diacyldigalactosyldiglycerides is considerably slower than that of the same label incorporated into bilayers of saturated phosphatidylcholines above the main phase transition. Differences between bilayers of diacyldigalactosyldiglycerides extracted from different plant membranes have been observed.

Introduction

Nitroxide spin probes are widely used in studies of the dynamic structure of membranes and lipid bilayer systems [1,2]. The spin-labelled derivative of 3α-cholestane, 3-doxylcholestane (CSL), has proved particularly useful as its ESR spectra reflect the overall motion of this rigid molecule. The CSL molecules are incorporated into the lipid bilayers with the steroid nucleus buried in the hydrophobic region and the nitroxide group located near the polar headgroups of the lipids [1,2]. The major axis of the hyperfine tensor is almost perpendicular to the long molecular axis and this affords the resolution of molecular reorientational motions both about the long molecular axis and perpendicular to it [2].

CSL incorporated into lipid bilayers exhibits a restricted anisotropic motion. However, the information about the orientational order and dynamics of the molecules cannot often be extracted in a straightforward manner from the observed ESR spectra [2,3]. This is particularly difficult in the slow-motion region, when the rotational correlation time, τ, characterizing the molecular dynamics is long on the ESR time scale, $\tau \gtrsim 2 \cdot 10^{-9}$ s. The problem has largely been overcome in recent years with the development of fast numerical algorithms for the solution of the stochastic Liouville equation which provides the basic description of the ESR spectra [4–6].

We have used the slow-tumbling ESR formalism [3–6] to analyse X-band ESR spectra of CSL incorporated into planar multibilayers of diacyldigalactosyldiglyceride (DGDG)/water mixtures. DGDG is an important component of

* To whom correspondence should be addressed.

thylakoid membranes of chloroplasts [7,8] and contains fatty acid chains with a high degree of unsaturation (about 70–80% 18 : 3 fatty acids). DGDG bilayers exhibit an order-disorder phase transition at low temperatures (approx. −50°C) [9,10] and have previously been characterized by X-ray diffraction [10]. We have considered the CSL molecules to undergo small-step stochastic reorientational diffusion, subject to a cylindrically symmetric orienting potential [3].

The simulations of the experimental spectra show that the slow-tumbling theory is indeed necessary for the analysis of the reorientational motion of the CSL molecules. In the temperature range −10°C–40°C, the long molecular axes were found to reorientate slowly ($D_\perp \approx 10^7$ s^{-1}), but the molecules undergo a much faster rotational motion around these axes ($D_\parallel \sim 4 \cdot 10^8$ s^{-1}). The CSL molecules possess furthermore a low degree of orientational order with respect to the bilayer normals, $\langle P_2 \rangle \sim 0.4$. This behaviour is in marked contrast to that observed for CSL molecules incorporated into bilayer systems composed of saturated phosphatidylcholines [11,12].

An interesting finding was that the ESR spectra obtained from multibilayers of DGDG extracted from spinach and curled kale chloroplasts exhibited different lineshapes from spectra recorded from bilayers of DGDG from cherry leaf chloroplasts. The differences can be almost wholly attributed to the lower degree of orientational order in the latter bilayer system. The decrease in order, however, is not accompanied by an increase in the rates of reorientational motion.

Materials and Methods

Digalactosyldiglyceride (DGDG) isolated from three sorts of leaves was used in this study. Purified DGDG from curled kale chloroplasts was obtained from Lipid Products (South Nutfield, U.K.), DGDG from spinach and cherry chloroplasts were prepared as described below. The solvents used (AR) were obtained from Baker and the cholestane spin label was purchased from Syva. Doubly distilled water was used throughout.

Purification of DGDG. The total lipid extraction from chloroplasts and subsequent fractionation in lipid classes was performed as described in Ref. 13. The acetone fraction obtained, containing mainly galactolipids, was purified further by preparative HPLC. A Lichrosorb Si-60-7 column (stainless steel, 250 × 22.7 mm, Chrompack Nederland, Middelburg, The Netherlands) was used. The column was eluted with chloroform/methanol (85 : 15, v/v). The fractions collected were analysed for purity on Silica gel 60 plates (10 × 10 cm, for nano-TLC, art. 5633, Merck, Darmstadt, F.R.G.). Chloroform/methanol/water (65 : 25 : 4, v/v) was used as the mobile phase. Only DGDG fractions containing no contaminants were used further.

Preparation of oriented multibilayers. DGDG and cholestane in molecular ratio of 125 : 1 were dissolved in chloroform/methanol (2 : 1, v/v). The solution was thoroughly mixed and the bulk of the solvent removed by evaporation under a stream of nitrogen. Residual solvent was removed by exposure to high vacuum. A small volume of water was then added to the dried mixture for a quick hydration. Oriented multibilayers were prepared by gently rubbing the hydrated lipid mixture between two microscope glass cover slips at room temperature. The alignment was monitored by a polarizing microscope.

Previous studies from our laboratory using optical techniques [25–30] have shown that polarization microscopy is a sensitive technique for monitoring the alignment of lipid multibilayers. It has been found that well oriented samples of DGDG can be obtained consistently with this preparation procedure, in marked contrast to phosphatidylcholine systems. The samples were subsequently equilibrated against a constant relative humidity of 98%. The hydration of the sample during ESR measurements was kept at the pre-equilibrated level by placing a saturated K_2SO_4 solution at the bottom of the tube in which the sample was mounted.

Oxidation of the lipids. As the polyunsaturated DGDG molecules are highly susceptible to oxidation, we have carried out the lipid isolation and multibilayer sample preparation strictly under a nitrogen atmosphere. The lipids came into contact with air for a short time during the alignment procedure under the polarizing microscope. The oxidation of the lipid molecules was monitored after every preparative step by recording their absorption spectrum in the 200–300 nm region [14]. Samples showing traces of peroxide forma-

tion were discarded. The ESR measurements were carried out on freshly prepared multibilayer samples.

A further indication of lipid oxidation was the loss in the intensity of the ESR signal. It has been previously shown [15] that spin-labels act as antioxidants in membrane systems. Consequently only those spectra obtained in experiments in which the ESR signal intensity decreased by less than 20% during the measurements were used further in the analysis. Furthermore, the reproducibility of the initial spectrum obtained in every series of experiments was checked at the end of the run. In general no changes in the spectral lineshapes were observed as a result of the loss of the ESR signal intensity.

Electron-spin resonance measurements. ESR measurements were carried out on a Varian E-9, X-band spectrometer equipped with a TM 110 cavity. The sample temperature was regulated with a Varian V4540 variable temperature accessory and measured with a copper-constantan thermocouple placed just above the sample.

The spectra were recorded at a microwave power level of 2 mW and a top-top modulation width of 1 G at 100 kHz was used. The sample could be oriented in the cavity by means of a goniometer. The orientation of the normal to the multibilayer surface relative to the applied static magnetic field is denoted by θ. Most of the spectra reported below were recorded for $\theta = 0°$.

The magnetic field strength was measured with a Bruker B-NM 12 NMR magnetometer and the microwave frequency was determined with a Hewlett-Packard HP5342A microwave frequency counter.

Spectral simulations. The simulations of the experimental ESR spectra were carried out by a numerical solution of the stochastic Liouville equation (SLE) following Moro and Freed [4]. The underlying theory has previously been extensively reviewed [3].

In solving the stochastic Liouville equation we assume that the cholestane spin-label molecules undergo a stochastic rotational diffusion subject to an anisotropic, cylindrically symmetric, orienting potential $U(\beta)$ [3].

$$U(\beta) = \varepsilon_2 P_2(\cos\beta) + \varepsilon_4 P_4(\cos\beta) \tag{1}$$

where β is the angle between the local director (the normal to the bilayer surface) and the long molecular axes of the spin labels. P_2 and P_4 denote Legendre polynomials of order 2 and 4.

The rotational diffusion tensor $\boldsymbol{D}$ is assumed to have a cylindrical symmetry about the molecular axes. It is characterized by the components $D_{\parallel}$ and $D_{\perp}$, respectively parallel and perpendicular to the long molecular axis.

The orienting potential $U(\beta)$ gives rise to an anisotropic distribution of the molecular axes [3]

$$f(\beta) = C\exp(\lambda_2 P_2 + \lambda_4 P_4) \tag{2}$$

where $\lambda_2 = -\varepsilon_2/\boldsymbol{kT}$ and $\lambda_4 = -\varepsilon_4/\boldsymbol{kT}$.
Here C is a normalizing constant such that

$$\int_0^{\pi} f(\beta)\sin\beta\,\mathrm{d}\beta = 1 \tag{3}$$

The orientational order parameters, $\langle P_L \rangle$, are given by

$$\langle P_L \rangle = \int_0^{\pi} f(\beta) P_L(\cos\beta)\sin\beta\,\mathrm{d}\beta \tag{4}$$

The range of possible values of λ_2 and λ_4 in Eqn. 2 can be restricted by noting that the nitroxide group of the cholestane molecules is anchored in the headgroup region of the bilayer [16]. It is expected from Eqn. 2 that $0 \leqslant \lambda_4 \leqslant 0.4\lambda_2$ so that the distribution function possesses a maximum at $\beta = 0°$ and decreases monotonically to a minimum at $\beta = 90°$. Furthermore, since we do not expect a priori a collective molecular tilt above the phase transition of the chains, we have $0 \leqslant -\lambda_4 \leqslant 0.3\lambda_2$.

The values for the components of the hyperfine $\boldsymbol{A}$ and $\boldsymbol{g}$ tensors were obtained from low-temperature spectra, on assuming that all molecular reorientational motions are effectively quenched. The corresponding powder spectra were simulated following [17].

The simulated spectra were convoluted with a Gaussian line, with a peak-to-peak width of the first derivative Δ_G, in order to account for the broadening caused by unresolved proton hyperfine interactions. It should be noted that homogeneous broadening enters the simulations through an effective electron spin-spin relaxation time T_{2e} [3–6].

Results

Low-temperature spectra

The values for the hyperfine A and g tensor components were determined from the 0° and 90° spectra (applied static field oriented along the normal to the multibilayers and perpendicular to it, respectively) at −29°C. The choice of the spectra at this temperature as powder spectra is somewhat arbitrary. The experimental and simulated spectra for curled kale chloroplasts DGDG are shown in Fig. 1a, together with those obtained from an unoriented dispersion of the lipids. The experimental and simulated 0° spectra for cherry leaf chloroplast DGDG are shown in Fig. 1b. The tensor components used in the simulations were: $A_{xx} = 0.59$ mT, $A_{yy} = 0.59$ mT, $A_{zz} = 3.39$ mT, $g_{xx} = 2.0082$, $g_{yy} = 2.0063$, $g_{zz} = 2.0024$.

We note here that the lineshapes of the simulated spectra are determined by the differences in the values of the components of the g-tensors and are not sensitive to their absolute values.

The distribution of molecular axes in the bilayers used in the simulations was described by Eqn. 2 with $\lambda_4 = 0$. The agreement between the simulated and experimental spectra improved only marginally on introducing either a P_4 dependence into Eqn. 2 or an angle-dependent linewidth.

Effect of model parameters on the simulated spectra

The lineshapes of the simulated 0°-spectra exhibit some characteristic dependences on the four model parameters $D_\perp$, $D_\parallel$, λ_2 and λ_4. These are illustrated in Fig. 2. A reference spectrum, marked as R in Fig. 2, similar to the experimental ones, was simulated with $D_\perp = 1 \cdot 10^7$ s^{-1}, $D_\parallel = 4 \cdot 10^8$ s^{-1}, $\lambda_2 = 1.6$ and $\lambda_4 = 0$. We note that here $D_\parallel$ falls within the motional-averaging limit, while $D_\perp$ lies in the slow-tumbling region.

On increasing λ_2 only, Fig. 2a, the relative intensities of the fine structure in the low-field and high-field parts of the spectrum change significantly. This can be attributed directly to the change in the contribution to the spectrum arising from the hyperfine A_{zz} component as a result of the increased orientational order.

The resolved structure in the lineshape disappears on increasing $D_\perp$, Fig. 2b top spectrum. However, this effect can be compensated by changing λ_2 and λ_4 simultaneously, Fig. 2b lower spectrum. In this way it is possible to change the ratio $D_\parallel/D_\perp$ without affecting the spectral lineshape.

It should be realized that, in general, the lineshapes can be changed dramatically on varying λ_2 and λ_4 which characterize the orientational order, Eqn. 2. However, as discussed above for our case of cholestane spin label molecules incorporated in

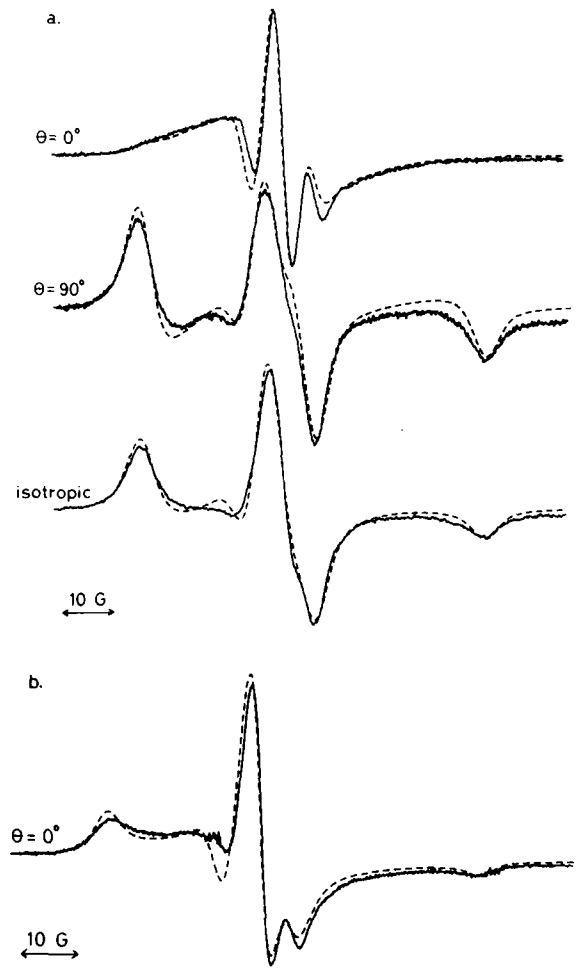

Fig. 1. Experimental spectra (———) at −29°C and calculated powder spectra (— — —). θ denotes the angle between the static magnetic field direction and the normal to the multibilayer plane. (a) DGDG from curled kale chloroplasts; $\lambda_2 = 2.8$, $\langle P_2 \rangle = 0.58$. The bottom spectrum was obtained from an isotropic bilayer dispersion. (b) DGDG from cherry chloroplasts; $\lambda_2 = 1.2$, $\langle P_2 \rangle = 0.26$. Broadening parameters used were: $T_{2e} = 2.5 \cdot 10^{-8}$ s for all the spectra; for $\theta = 0°$, $\Delta_G = 2.2$ G; for $\theta = 90°$ and isotropic spectrum $\Delta_G = 3.2$ G.

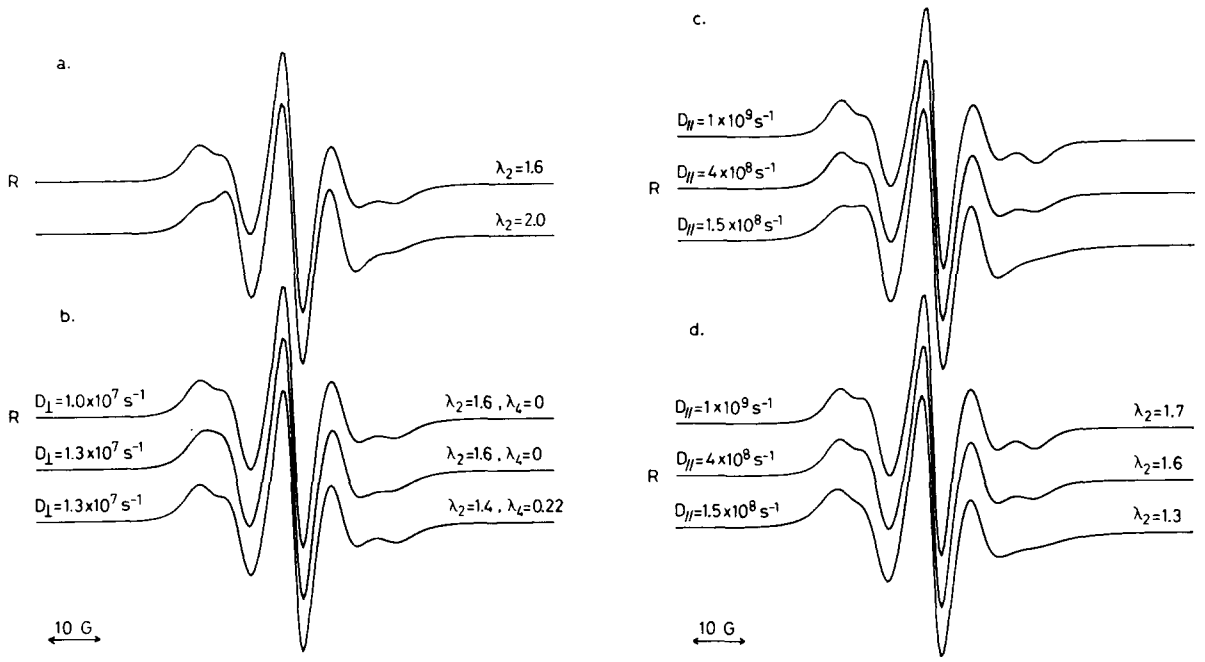

Fig. 2. Simulated 0°-spectra illustrating the dependence of the lineshape on the model parameters λ_2, λ_4, $D_{\parallel}$ and $D_{\perp}$. The reference spectrum marked by R was calculated with $D_{\perp} = 1 \cdot 10^7\ s^{-1}$, $D_{\parallel} = 4 \cdot 10^8\ s^{-1}$, $\lambda_2 = 1.6$ and $\lambda_4 = 0.0$. The values of the parameters that are varied are shown next to the spectrum. The values of the other parameters are the same as those for the reference spectrum R. For all the spectra $T_{2e} = 6.6 \cdot 10^{-8}$ s and $\Delta_G = 2.2$ G.

membrane systems, the range of values of these parameters can be restricted considerably. In the main, a small change in λ_4 has a similar effect on the spectrum as a small change in λ_2. Furthermore, an increase in λ_2 and a simultaneous decrease in λ_4 by the same amount leaves the peak positions unaltered, but enhances the structure in the lineshape.

The influence of $D_{\parallel}$ on the spectra is shown in Fig. 2c. An increase in $D_{\parallel}$ results in a narrowing of the spectral components, with a concomitant sharpening of the structures on the low- and high-field parts. A decrease in $D_{\parallel}$ causes a broadening of these features of the spectrum.

The changes in the lineshape brought about on changing $D_{\parallel}$ can be compensated to a large degree by changing λ_2 simultaneously, Fig. 2d. The shape of the low field lines can thus be kept almost constant, while the high field lines change form. This correlation between $D_{\parallel}$ and λ_2 weakens considerably if $D_{\parallel}$ is so reduced that it lies in the slow-tumbling regime.

Simulations of the slow-motion spectra

Because the effects of the model parameters on the simulated lineshapes tend to be correlated, we have chosen to simulate the experimental spectra using the simplest potential function, Eqn. 1, with $\epsilon_4 = 0$. The spectra obtained from curled kale chloroplast DGDG and cherry chloroplast DGDG are shown, respectively, in Figs. 3 and 4 together with the best simulations. The model parameters used in the calculations are given in Tables I and II.

It can be seen from Fig. 3 that the agreement between the experimental and simulated spectra is good at high temperatures, but worsens progressively with decreasing temperature. A similar effect is also observed for the cherry chloroplast DGDG, Fig. 4. The discrepancies can only be marginally improved if the term in ϵ_4, Eqn. 1, is introduced into the calculations. The spectral lineshapes from bilayers of curled kale DGDG at temperatures below -8°C appear, furthermore, to be rather insensitive to the choice of the model parameters. We have also been unable to simulate

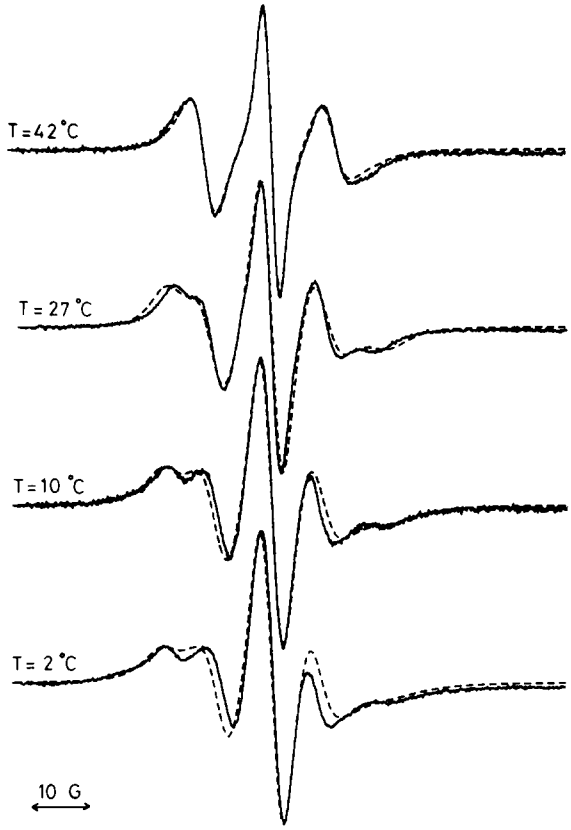

Fig. 3. Experimental (———) and calculated (— — —) 0° spectra of cholestane in multibilayers of DGDG from curled kale chloroplasts. The relevant model parameters are given in Table I. For the spectrum at 42°C, $D_{\parallel} = 1 \cdot 10^{9}\ s^{-1}$ and $\Delta_G = 1.8$ G. For the other spectra $\Delta_G = 2.2$ G. Values for T_{2e} from top to bottom: $3 \cdot 10^{-7}$ s, $6.6 \cdot 10^{-8}$ s, $4.7 \cdot 10^{-8}$ s and $4.4 \cdot 10^{-8}$ s.

spectra satisfactorily for cherry chloroplasts DGDG at temperatures below 18°C. It is interesting to note the large differences between the experimental spectra obtained from bilayers of curled kale and cherry chloroplasts DGDG. The spectra from bilayers of spinach DGDG (not shown) were almost identical with those obtained from curled kale DGDG bilayers.

The results from the simulations of the curled kale DGDG spectra, Table I, show that for $t \gtrsim 10$°C, the values for $D_{\parallel}$ lie in the fast-motional region, while the values for $D_{\perp}$ correspond to the slow-motion regime. It appears that the ratio $D_{\parallel}/D_{\perp} \approx 40$–$50$ throughout the temperature range studied. At temperatures below ≈ 10°C, the motional rates slow down so that both components of the diffusion tensor have values corresponding to the slow-tumbling region. The orientational order of the long molecular axes, as reflected in λ_2 and hence $\langle P_2 \rangle$, is fairly low and does not change markedly: $\langle P_2 \rangle$ increases from ≈ 0.36 at 42°C to ≈ 0.42 at -8°C. A comparison of Table I and II shows that the differences between the curled kale

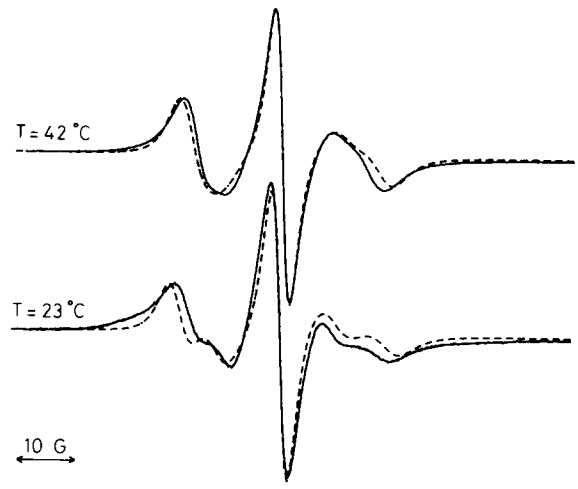

Fig. 4. Experimental (———) and calculated (— — —) 0° spectra of cholestane in multibilayers of DGDG from cherry chloroplasts. The model parameters are given in Table II. $T_{2e} = 3 \cdot 10^{-7}$ s and $\Delta_G = 2.1$ G for all the spectra.

TABLE I

PARAMETERS USED IN THE SIMULATION OF X-BAND SPECTRA FROM CHOLESTANE SPIN LABEL IN ORIENTED MULTIBILAYERS OF CURLED KALE CHLOROPLAST DGDG AT VARIOUS TEMPERATURES

T (°C)	$D_{\perp}$ (s^{-1}) [a] ($\times 10^{-7}$)	$D_{\parallel}$ (s^{-1}) [b] ($\times 10^{-8}$)	λ_2 [c]	ε_2 (joules) [d] ($\times 10^{21}$)	$\langle P_2 \rangle$
42	2.5	> 5 [e]	1.6	−7.0	0.36
36	2.0	> 5 [e]	1.6	−6.8	0.36
27	1.0	4	1.6	−6.6	0.36
18	0.8	3	1.7	−6.8	0.38
10	0.5	2	1.8	−7.0	0.40
2	0.3	1.5	1.9	−7.2	0.42
−8	0.2	1.0	1.9	−6.9	0.42

[a] Error $\pm 2 \cdot 10^{6}$.
[b] Error $\pm 25\%$.
[c] Error ± 0.1.
[d] Error $\pm 4 \cdot 10^{-22}$.
[e] The spectral shape is insensitive to $D_{\parallel}$ for $D_{\parallel} \geq 10 \cdot D_{\perp}$.

TABLE II

PARAMETERS USED IN THE SIMULATION OF X-BAND SPECTRA FROM CHOLESTANE SPIN LABEL IN ORIENTED BILAYERS OF CHERRY CHLOROPLAST DGDG AT VARIOUS TEMPERATURES

T (°C)	$D_\perp$ (s^{-1}) [a] ($\times 10^{-7}$)	$D_\parallel$ (s^{-1}) [b] ($\times 10^{-8}$)	λ_2 [c]	ε_2 (joules) [d] ($\times 10^{21}$)	$\langle P_2 \rangle$
42	1.8	6	0.7	−3.0	0.15
33	1.2	4	0.6	−2.5	0.13
27	1.0	3.5	0.7	−2.9	0.15
23	0.7	3	0.8	−3.3	0.17
18	0.5	2	0.8	−3.2	0.17

[a] Error $\pm 2 \cdot 10^6$.
[b] Error $\pm 25\%$.
[c] Error ± 0.1.
[d] Error $\pm 4 \cdot 10^{-22}$.

and cherry DGDG bilayers arises mainly from the marked differences in the orientational ordering of the spin-label molecules. The values of $\langle P_2 \rangle$ for cherry DGDG bilayers are roughly half those obtained for the curled kale DGDG bilayers and furthermore only show a slight temperature dependence. It is interesting to note that here the reduction in orientational order is not accompanied by higher rates of molecular motion.

Discussion

We have here presented ESR spectra of cholestane spin-label molecules incorporated into multibilayers of DGDG extracted from different plant species. The spectra were simulated in terms of the formalism for slow-tumbling developed by Freed and his co-workers [3]. We have assumed that the cholestane molecules undergo small-step stochastic diffusion subject to the action of a cylindrically symmetric orienting potential. We have found that the experimental 0°-spectra presented could be adequately described by the so-called Maier-Saupe potential, $U(\beta) = \varepsilon_2 P_2(\cos \beta)$. Nevertheless we note that our simulations indicate that the effects of the model parameters on the spectral lineshapes are correlated. Thus the use of a different functional form for the orienting potential will modify the quoted values for the diffusion coefficients $D_\parallel$ and $D_\perp$.

The simulations show that the slow-tumbling theory must indeed be applied for the interpretation of the ESR spectra obtained from our systems. The values of $D_\perp$ obtained, even from the simulations of the three line spectra recorded around 40°C, correspond to the slow-tumbling time regime. The simulations of the spectra obtained for $t \lesssim 25$°C, are insensitive to the values of $D_\perp$ as the reorientational motion of the long axes of the cholestane molecules becomes extremely slow on the ESR time scale. In contrast, the rotational rates about the long molecular axes fall within the fast-motional regime for $t \gtrsim 10$°C. Indeed these motions are so fast in bilayers of curled kale and spinach DGDG for $t \gtrsim 36$°C, that only a lower limit of $D_\parallel$ can be obtained from the 0° spectra.

The ambiguities in the absolute values of the rotational diffusion coefficients obtained from analysis of the 0° spectra could well be removed by a full study of the angle-dependence of the spectral lineshapes. This work is now in progress. Nevertheless, the results presented here show unequivocably that the spin-label molecules undergo a much faster reorientational motion about their long molecular axes than perpendicular to them.

The assumption of a cylindrically symmetric orienting potential may well be valid for simulations at high temperatures where the rotations about the long molecular axes are fast enough to effectively average the anisotropies of the hyperfine $\boldsymbol{A}$ and $\boldsymbol{g}$ tensors. The discrepancies between the experimental and simulated spectra observed at low temperatures could be due to the breakdown of this assumption as a result of slower reorientational motions. Furthermore, we have assumed in common with previous workers that the long axis of the cholestane molecule is perpendicular to the plane of the oxazolidine ring. However, as noted in Ref. 18 the angle between the normal to the ring and the long molecular axis lies in the region of 100°–110°. This will also contribute to the disagreement between the experimental and simulated spectra.

The experimental spectra exhibit a marked structure, or splitting, on the low-field side. These lineshapes can be reproduced by the model used in our simulations. The calculations indicate that in the slow-tumbling regime such a splitting arises from the low orientational ordering of the long

molecular axes relative to the normal to the plane of the multibilayers. We conclude, therefore, that the observation of such a composite lineshape does not necessarily imply the existence of domains of different properties in the sample.

An inspection of Tables I and II shows that for both DGDG systems the ratio $D_{\parallel}/D_{\perp} \approx 40-50$ is virtually temperature independent. Similar ratios have also been obtained for cholestane spin labels in thermotropic liquid-crystalline mesophases [18]. However, a consideration of the moments of inertia of the molecule for rotation about its centre of mass lead to $D_{\parallel}/D_{\perp} \sim 4.7$ [19].

As the cholestane molecule is anchored with the oxazolidine ring in the headgroup region of the membrane we expect the ratio of the moments of inertia to increase. On taking the molecule to be a uniform rod, it can be shown from the parallel-axis theorem that the ratio of the moments of inertia will increase by a factor of 4, so that $D_{\parallel}/D_{\perp} \approx 20$. This ratio is significantly lower than that yielded by the simulations. One reason for the discrepancy may be found in our choice of the functional form of the orienting potential as discussed above. On the other hand, it is known that the rotational behaviour of small anisotropic molecules in simple liquids approximates a slipping rather than the sticking boundary condition of classical hydrodynamic theory [20–22]. This effect could also explain our results. It can be reasoned intuitively that the motion of the long molecular axes of the cholestane molecules, characterized by $D_{\perp}$ may involve cooperative motions of the lipid molecules in the bilayer. On the other hand, the rotation about the long axes, leading to $D_{\parallel}$, is less hindered. It only involves motion among the surrounding lipid chains which themselves undergo fast rotations about their long axes.

An interesting conclusion of this work is that the differences in the spectra obtained from multilayers of DGDG from cherry chloroplasts on the one hand and spinach and curled kale chloroplasts on the other, can be almost wholly attributed to a different degree of orientational ordering. The orienting potential is significantly lower in the former system than in the latter ones. This decrease in order, however, is not accompanied by an increase in the rates of reorientational motions, as reflected in the values of $D_{\parallel}$ and $D_{\perp}$. The reason for this behaviour is not clear. We note that although the same ESR spectra are obtained from bilayers of DGDG from spinach and curled kale chloroplasts, the two lipids have a different fatty acid composition. DGDG from spinach chloroplasts contains 87% 18 : 3 fatty acid chains with small amount of 18 : 1, 16 : 3 and 16 : 0 chains [23], while DGDG from curled kale chloroplasts contains only 46% 18 : 3 chains with 14% each of 18 : 2, 18 : 1 and 16 : 1 chains [24]. We have been unable to find any reports of the fatty acid composition of DGDG from cherry leaf chloroplasts. This point must be investigated further.

The ESR spectra reported here for the unsaturated lipid DGDG are markedly different from those obtained for the same label incorporated into multibilayers of saturated phosphatidylcholines and egg phosphatidylcholine [11,12]. Our simulations indicate that this difference arises to a large degree from the slower reorientational motions of the label in DGDG multibilayers. A similar conclusion has also been reached in other studies in our laboratory, using fluorescence depolarization techniques [25,26]. In these studies the fluorescent molecule 1,6-diphenylhexatriene (DPH) was used as a probe. These results thus contradict the generally accepted picture that the introduction of unsaturation into the hydrocarbon chains of lipid molecules increases their fluidity. Our findings suggest that both the degree of orientational ordering and the rates of molecular motions are lowered. This point is being studied further in our laboratory.

References

1 Berliner, L.J. (1976) Spin Labeling, Theory and Applications, Academic Press, New York
2 Hemminga, M.A. (1983) Chem. Phys. Lipids 32, 323–372
3 Freed, J.H. (1976) in Spin Labeling, Theory and Applications (Berliner, L.J., ed.), Ch. 3, Academic Press, New York
4 Moro, G. and Freed, J.H. (1981) J. Chem. Phys. 74, 3757–3773
5 Dammers, A.J., Levine, Y.K. and Tjon, J.A. (1982) Chem. Phys. Lett. 88, 198–201
6 Giordano, M., Grigolini, P., Leporini, D. and Marin, P. (1983) Phys. Rev. A28, 2474–2481
7 Quinn, P.J. and Williams, W.P. (1983) Biochim. Biophys. Acta 737, 223–266
8 Douce, R. and Joyard, J. (1980) in The Biochemistry of Plants, Vol. 4, pp. 321–362, Academic Press, New York

9 Quinn, P.J., (1981) Progr. Biophys. Mol. Biol. 38, 1–104
10 Shipley, G.G., Green, J.P. and Nicholas, B.W. (1973) Biochim. Biophys. Acta 311, 531–544
11 Smith, I.C.P. and Butler, K.W. (1976) in Spin Labeling, Theory and Applications (Berliner, L.J., ed.), Ch. 11, Academic Press, New York
12 Ehrström, M. and Ehrenberg, A. (1983) Biochim. Biophys. Acta 735, 271–282
13 Fork, D.C., Van Ginkel, G. and Harvey, G. (1981) Plant Cell Physiol. 22, 1035–1042
14 Klein, R.A. (1970) Biochim. Biophys. Acta 210, 486–489
15 Hicks, M. and Gebicki, J.M. (1981) Arch. Biochem. Biophys. 210, 56–63
16 Schreier-Mucilli, S., Marsh, D. and Smith, I.C.P. (1976) Arch. Biochem. Biophys. 172, 1–11
17 Hemminga, M.A. (1977) J. Magn. Reson. 25, 25–45
18 Carr, S.G., Khoo, S.K., Luckhurst, G.R. and Zannoni, C. (1976) Mol. Cryst. Liq. Cryst. 35, 7–13
19 Rao, K.V.S., Polnaszek, C.F. and Freed, J.H. (1977) J. Phys. Chem. 81, 449–456
20 Dote, J.L., Kivelson, D. and Schwartz, R.N. (1981) J. Phys. Chem. 85, 2169–2180
21 Jones, L.L. and Schwartz, R.N. (1981) Mol. Phys. 43, 527–555
22 Bauer, D.R., Alms, G.R., Brauman, J.I. and Pecora, R. (1974) J. Chem. Phys. 61, 2255–2261
23 Douce, R., Holz, R.B. and Benson, A.A. (1973) J. Biol. Chem. 248, 7215–7222
24 Hudson, B.J.F. and Karis, I.G. (1974) J. Sci. Food Agric. 25, 1491–1502
25 Van de Ven, M.J.M. (1983) Thesis, University of Utrecht
26 Van de Ven, M.J.M. and Levine, Y.K. (1984) Biochim. Biophys. Acta 777, 283–296
27 Van de Ven, M.J.M., Kattenberg, M., Van Ginkel, G. and Levine, Y.K. (1984) Biophys. J. 45, 1203–1210
28 Vos, M.H., Kooyman, R.P.H. and Levine, Y.K. (1983) Biochem. Biophys. Res. Commun. 116, 462–468
29 Kooyman, R.P.H., Vos, M.H. and Levine, Y.K. (1983) Chem. Phys. 81, 461–472
30 Van de Ven, M.J.M., Kattenberg, M., Van Ginkel, G,, Verver, W. and Levine, Y.K. (1984) Biochem. Biophys. Res. Commun. 120, 1060–1066